Discovery of Novel Nitrobenzothiazole Inhibitors for *Mycobacterium tuberculosis* ATP Phosphoribosyl Transferase (HisG) through Virtual Screening

Yoonsang Cho,[†] Thomas R. Ioerger,*[,‡] and James C. Sacchettini[§]

Department of Pharmacology, Yale University School of Medicine, New Haven, Connecticut, Department of Computer Science, Texas A&M University, 218 Biochemistry and Biophysics Building, TAMUS 2128, College Station, Texas 77840-212, Department of Biochemistry and Biophysics, Texas A&M University, College Station, Texas

Received March 21, 2008

HisG is an ATP-phosphoribosyl transferase (ATPPRTase) that catalyzes the first step in the biosynthetic pathway for histidine. Among the enzymes in this pathway, only HisG represents a potential drug target for tuberculosis. Only a few inhibitors with limited potency for HisG are currently known. To discover more potent and diverse inhibitors, virtual screening was performed. The crystal structure of *M. tuberculosis* HisG has been solved and reveals a large, solvent-exposed active site with subsites for ATP and PRPP substrates. Two docking algorithms, GOLD and FLEXX, were used to screen two large libraries, Chembridge and NCI, containing over 500000 compounds combined. An initial subset of top-ranked compounds were selected and assayed, and seven were found to have enzyme inhibition activity at micromolar concentrations. Several of the hits contained a nitrobenzothiazole fragment, which was predicted to dock into the monophosphate-binding loop, and this binding mode was confirmed by crystallographic evidence. A secondary screen was performed to identify compounds with similar structures. Several of these also exhibited micromolar inhibition. Furthermore, two of the compounds showed bacteriocidal activity in a whole-cell assay against *Mycobacterium smegmatis*.

Introduction

HisG is an ATP-phosphoribosyl transferase (ATP-PRTase[a]) that catalyzes the first step in the biosynthetic pathway for histidine, which also leads to intermediates that play a role in purine biosynthesis. HisG condenses ATP with phosphoribosyl pyrophosphate (PRPP) to produce phosphoribosyl ATP (PR-ATP) and inorganic pyrophosphate (PP_i) (see Figure 1). Histidine biosynthesis is metabolically expensive, requiring 10 enzymatic reactions and consuming an estimated 41 ATP molecules. Therefore, the pathway is tightly regulated through negative feedback via allosteric inhibition of HisG by histidine.[1]

Partly because of its central role in metabolism and its uniqueness to prokaryotes and lower eukaryotes (not present in humans), HisG represents a potential drug target for combating tuberculosis. Tuberculosis kills over 2 million people per year worldwide, and it is estimated that over one-third of the human population is at least latently infected. New antitubercular drugs are needed because of the lengthy treatment course (standard DOTS therapy prescribes a regimen of four front-line drugs over six months) and more importantly because of the alarming rise of drug-resistant (MDR/XDR) strains.[2]

One reason HisG makes a good potential drug target is that it has been shown to be essential for growth in vitro using transposon-insertion (TraSH) experiments.[3] Although HisG knockouts have not been reported in the literature, deletion mutants for other enzymes in the histidine biosynthesis pathway have been constructed. Parish[4] showed that a *HisDC*$^-$ knockout is auxotrophic for histidine, reflecting the essentiality of this pathway and uniqueness of its intermediates. Moreover, infection of macrophages by the *HisDC*$^-$ mutant was significantly attenuated compared to wild-type (H37Rv). Core metabolite biosynthetic pathways such as for histidine are thought to be important for survival of mycobacteria in vivo due to possible nutrient-limiting conditions that develop during sequestration within macrophage phagosomes.[5]

The crystal structure of HisG has been solved in several organisms, including *Mycobacterium tuberculosis*[6] and *Escherichia coli*,[7] along with several other Eubacteria.[8,9] The molecular architecture of HisG is distinct from other phosphoribosyltransferase families (e.g., hypoxanthine-guanine PRTase and many others involved in purine and pyrimidine biosynthesis[10]) and is categorized as a unique type IV PRTase fold. Two forms of HisG exist: a "short" form of ~200 amino acids, and a "long" form of ~300 amino acids. The shorter homologs form a hetero-octamer with HisZ, a regulatory partner. In cotrast, the longer homologs form a homohexamer lacking HisZ. *Mtb* is a member of the latter group (i.e., long form of HisG; HisZ homologue absent from genome), as is *E. coli*.

HisG in *Mtb* has an α/β fold containing three domains: two N-terminal catalytic domains, with a large, relatively solvent-exposed active site formed between them, and a C-terminal regulatory domain.[6] The active site is formed by residues contributed by both domains I and II and contains putative binding sites for both ATP and PRPP, inferred based on co-crystal structures of complexes with AMP, PRPP, and PR-ATP (product).[6−8] Domain II contains a 13-residue signature sequence (residues 149−161) associated with binding PRPP (including a classic monophosphate-binding loop affording hydrogen-bonding to backbone atoms), whereas conserved residues for ATP-binding are primarily found in domain I on the opposing face of the cleft. While the reaction mechanism

* To whom correspondence should be addressed. Phone: (979)862-7636. Fax: (979)862-7638. E-mail: ioerger@cs.tamu.edu.
[†] Department of Pharmacology, Yale University School of Medicine.
[‡] Department of Computer Science, Texas A&M University.
[§] Department of Biochemistry and Biophysics, Texas A&M University.

[a] Abbreviations: AMP, adenosine monophosphate; ATP, adenosine triphosphate; DMSO, dimethyl sulfoxide; DOTS, daily observed therapy short course; NBT, nitrobenzothiazole; PRPP, phosphoribosyl pyrophosphate; PRTase, phosphoribosyltransferase, MDR, multidrug resistant; XDR, extreme multidrug resistant; IC_{50}, 50% inhibitory concentration; MIC, minimal inhibitory concentration; K_i, inhibition (dissociation) constant.

10.1021/jm800328v CCC: $40.75
Published on Web 09/09/2008

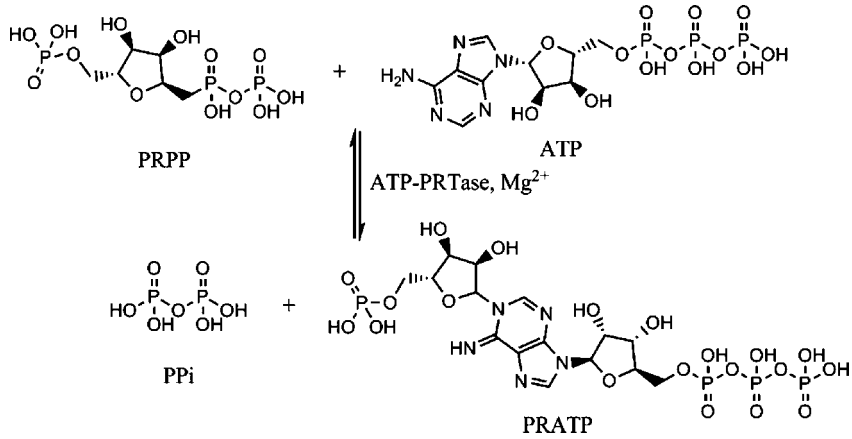

Figure 1. ATP phosphoribosyl transferase reaction catalyzed by HisG.

has not yet been completely determined, it follows ordered bi−bi kinetics, with sequential binding of ATP followed by PRPP, condensation, and then release of products PP_i and PR-ATP.[11] The C-terminal domain (III) binds histidine at a site approximately 40 Å away from the active site, which causes a rotation between domains and a conformational shift in packing within the hexameric complex,[6]which ultimately inhibits catalytic activity by reducing k_{cat}.[12]

To date, only a few inhibitors for HisG have been identified. AMP is a competitive inhibitor for both substrates, with a K_i of 550 μM.[13] Pentachlorophenol, dicoumarol, and 2,4-dinitrophenol have all been shown to have moderate inhibition strengths, with K_i's in the range of 50−400 μM against the *E. coli* enzyme.[14] Three-dimensional pharmacophore searching was used to identify biaryl inhibitors of *Arabidopsis thaliana* HisG, the most potent of which was a di(amino-naphthyl)-disulfide with an IC_{50} of 50 nM.[15] In this study, we report the results of a virtual screen for novel inhibitors for HisG. An initial screen yielded several hits that had significant inhibition in an in vitro assay, with IC_{50}'s in the 1−10 μM range. One of the strongest of these contained a nitrobenzothiazole (NBT) group, which virtual SAR (docking of related compounds) suggested was the substituent critical to the efficacy of the binding. Diffraction data collected from a co-crystal confirmed that the NBT packs in the part of the active site responsible for binding the PRPP substrate, as predicted by the docking, and the affinity can be rationalized through a network of hydrophobic and hydrogen-bonding interactions. Chemical similarity searches based on the NBT fragment and subsequent docking yielded several more hits that also had IC_{50}'s in the low-micromolar range. Two of these showed bacteriocidal whole-cell activity when tested on the related strain *Mycobacterium smegmatis*. These results open up a new avenue of possibilities for drug design for tuberculosis, specifically through inhibitors of HisG.

Methods

Virtual Screening. Two-dimensional chemical structures from the libraries were converted to 3D structures using CONCORD in the Sybyl package (Tripos, Inc.) and were assigned partial charges by the Gasteiger−Marsili method. Two separate docking algorithms were used for screening virtual compound libraries: GOLD and FlexX. These algorithms were validated by docking the product, PR-ATP, into the active site and showing that it docks in the expected position (based on the crystal structure of the complex with the *E. coli* ATP-PRTase, PDB: 1Q1K). Initial screens were performed by docking each molecule in a database with GOLD[16] using distributed computing on a computational grid. The receptor was prepared based on PDB 1NH8 (complex with AMP and histidine), with all ligands and water molecules removed and with hydrogens added (using Sybyl). The active site was centered on the Tyr116, which is thought to interact with ATP, and included residues within a radius of 15 Å, encompassing residues 157−159

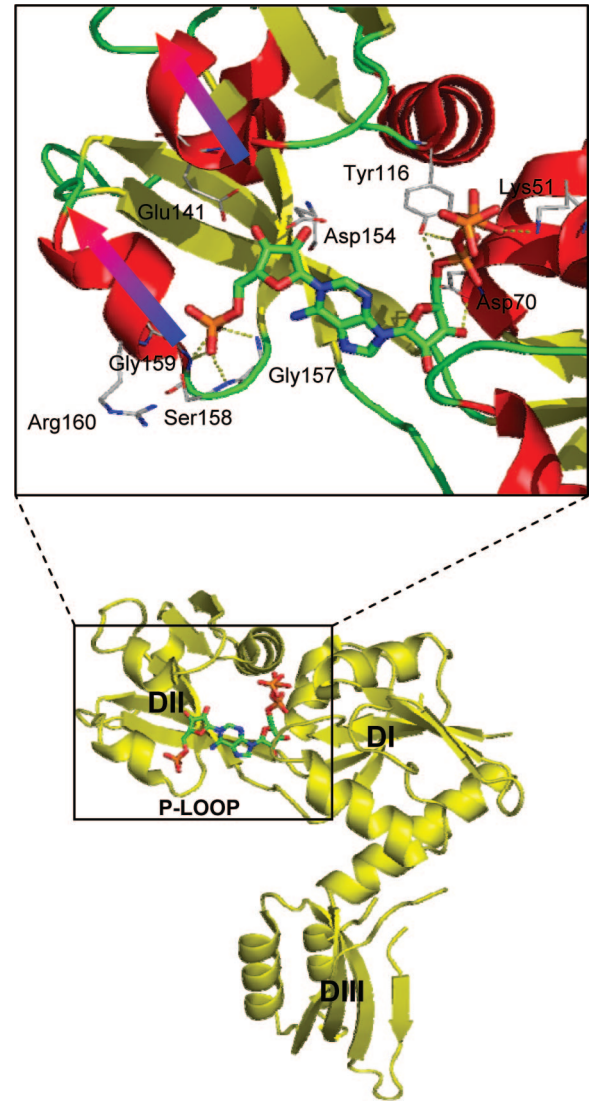

Figure 2. Skeleton of active site complexed with AMP (PDB: 1NH8), highlighting the P-loop (Gly157-Ser158, Gly159) and putative Mg:PRPP binding site (Asp154, Glu141, Ala139). A model of the product, PRATP, is shown in the active site to illustrate interaction with important residues.

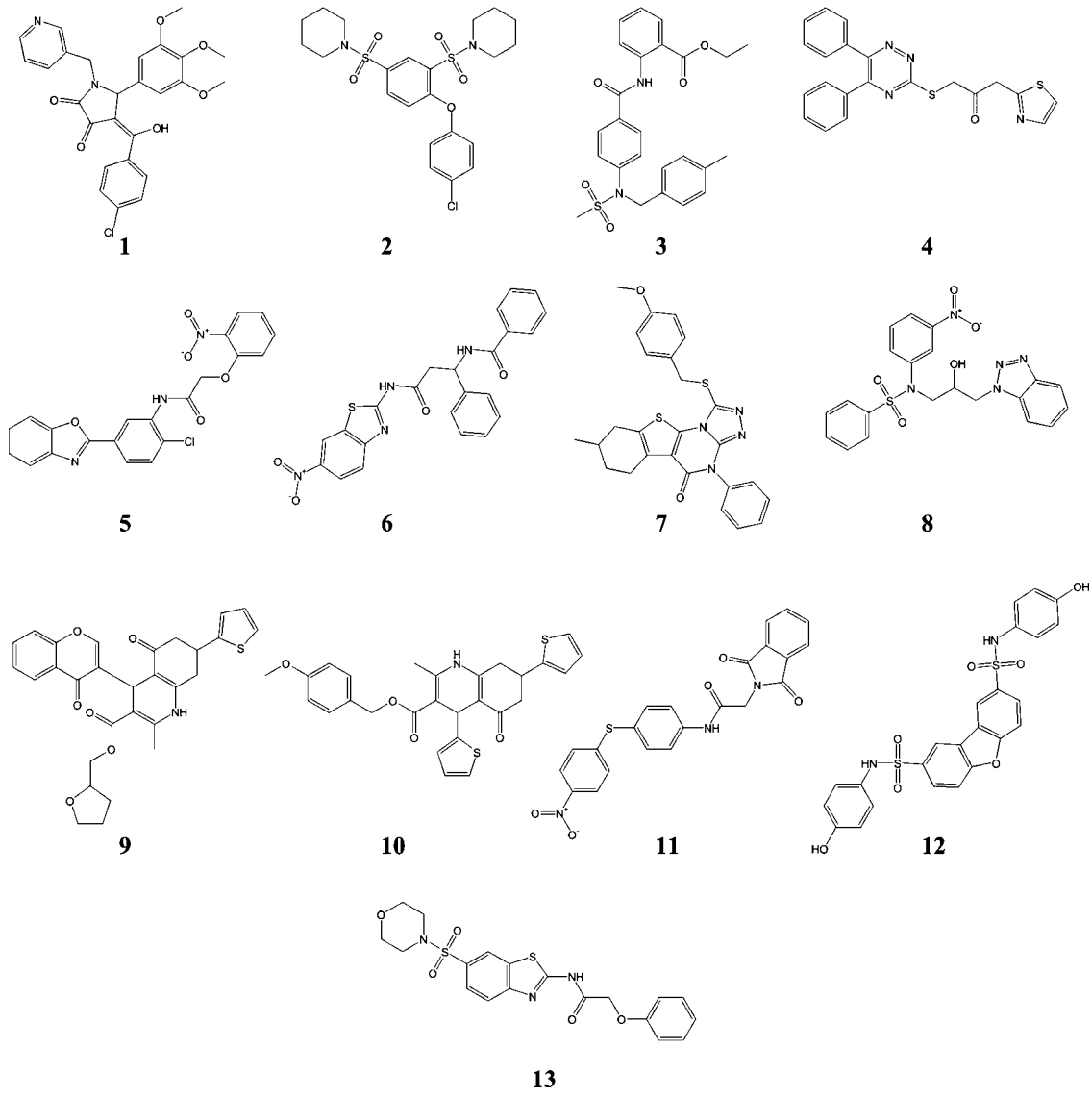

Figure 3. Structures of compounds selected from ChemBridge library based on initial screen.

(P-loop), along with Glu141 and Asp154, which are expected to interact with PRPP. Top conformers for each compound were scored and ranked with the GOLD energy score. To carry out the docking of hundreds of thousands of molecules in large databases, molecules in groups of 100 were distributed on a grid of approximately 350 computers (networked PCs) using grid-computing software from United Devices (Austin, TX), which automated the assignment of jobs and retrieval of results.

Subsequently, selected molecules were redocked with FlexX[17] and reranked using Consensus Scoring, as implemented in Sybyl (version 6.91). The receptor files were prepared in a similar way as for GOLD. Once docked, each molecule was assigned a FlexX score using the built-in function for interaction energy. Then scores based on four alternative energy functions were computed for the top conformer of each, as implemented in Sybyl: DOCK,[18] Chemscore,[19] PMF,[20] and GOLD.[21] The five scores were combined using Consensus Scoring[22] to rerank molecules based on how many times they were ranked in the top 50% according to each individual score. Cerius2 (Accelrys, Inc.) was used to evaluate drug-likeness of candidate molecules, calculate properties such as logP, and apply Lipinski's Rules[23] to filter hits.

Enzyme Assay. Inhibition activity was determined using an assay that followed the production of PR-ATP spectrophotometrically.[11] To evaluate inhibition activity of compounds against the HisG enzyme, 10 mM stocks of each molecule were prepared in DMSO. A reaction mixture (300 μL) was prepared with the same formula optimized for enzyme activity (0.1 M Tris-HCl pH 8.5, 0.15 M KCl, 20 mM NaCl, 0.25 mM ATP, and 3 units of inorganic pyrophosphatase from yeast) with 10 μM of testing compound. The reaction mixture was incubated for 10 min at ambient temperature. Enzymatic reaction was triggered by adding the substrate PRPP (0.25 mM), and absorbance of product was monitored at 290 nm for 5 min until it formed a plateau. DMSO was found not to interfere with the assay.

X-ray Crystallography. Inhibitor soaks were performed with apocrystals grown in the original condition (0.1 M MES pH 6.5, and 1.7 M $MgSO_4$). Stock solutions of compounds were solublized in DMSO at 10 mM. A single apo-crystal was transferred to 5 μL of mother liquor, followed by adding 1 mM of testing compound. The crystal was then incubated at 16 °C for 48 h. Diffraction data was collected on a Nonius/MAC-Science DIP2030 image plate detector with a RIGAKU rotating anode X-ray generator and was indexed and scaled by HKL2000.[24] The cell parameters were isomorphous with those of the apocrystal: space group $R32$, $a = b = 131.3$ Å and $c = 109.7$ Å, $\alpha = \beta = 90°$ and $\gamma = 120°$. Phases were determined by molecular replacement using Phaser,[25] with the apostructure (1NH7) as the search model. The structural model was refined initially by CNS[26] and then by Refmac5[27] via CCP4i.

Whole-Cell Assay. To determine the bacteriocidal properties of candidate compounds, a whole-cell assay was used to evaluate growth-inhibition of *M. smegmatis* (American Type Culture Col-

(a)

compound id		% Inh @ 10 μM	IC_{50}
4	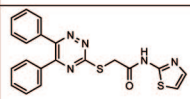	76%	4 μM
6	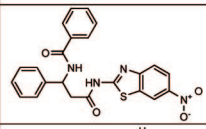	71%	6 μM
14	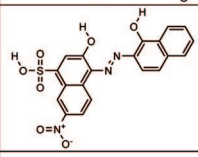	50%	~10 μM
10	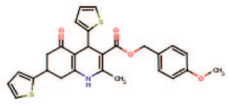	50%	~10 μM
15	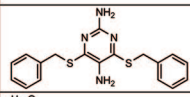	48%	n.d.
16	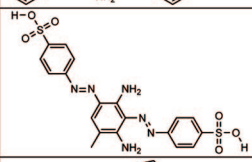	45%	n.d.
1	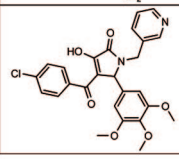	20%	n.d.

(b)

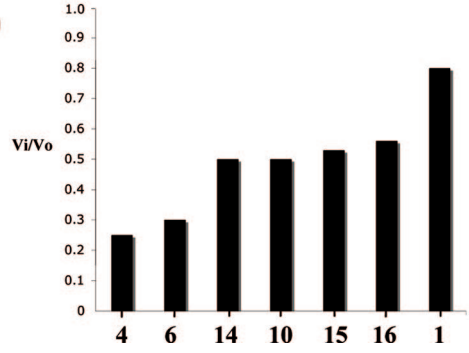

Figure 4. Enzyme inhibition for compounds selected from the ChemBridge and NCI databases in the initial virtual screen that showed inhibition activity. (a) Chart showing structures of compounds with inhibition activity, along with estimates of IC_{50}. n.d. = not determined. (b) Plot showing percent inhibition, as measured by the ratio of initial velocity of reaction with inhibitor (v_i) relative to velocity of control (v_o).

lection (ATCC) ID: 700084). The bacteria were grown in modified mycobacterium media (7H9 medium from BD Co. with 0.2% glucose and 0.05% Tween 80) for two days. The surfactant Tween 80 was added to the liquid culture to facilitate dispersion of mycobacteria. Agar-containing media (7H10 from BD Co. with 0.2% glycerol) was autoclaved and thoroughly mixed with different amounts (1, 3, 6, 12, and 25 μg/mL, respectively) of candidate compounds and allowed to solidify. Plates were treated with 25 μg/mL of kanamycin as a positive control. Also, 100 μL of DMSO was added to the medium and tested for interference with the ATP-PRTase activity. The culture plates were incubated at 37 °C for 4 days until the bacteria grew enough to judge growth inhibition by the molecules.

Results

Virtual Screening. A multistage strategy was chosen for virtual screening to identify inhibitors for HisG. First, two large, publically available chemical databases with a total of over 500000 compounds were searched by docking with GOLD, in a distributed fashion on a computational grid. Then approximately 1% of the top-ranked compounds were selected and redocked with FlexX and reranked using Consensus Scoring. The databases that were searched were: ChemBridge (CB) Express Pick (http://chembridge.com) and the National Cancer Institute (NCI) Open database (http://cactus.nci.nih.gov/ncidb2/download.html), with 350000 and 250000 compounds, respectively. The compound files were prepared, along with the receptor files for the active site, as described in the Methods section.

These two databases of compounds were first docked with GOLD. Using a computational grid of 350 networked computers (taking 32 h to dock the entire ChemBridge database using GOLD, and similar for the NCI database). The docked conformations were evaluated by their GOLD scores, which were used to compile a preliminary ranked list. Many of the top-ranked hits made multiple (>3) hydrogen bonds with the active site and matched well sterically with the binding surface. Some unusually highly scored molecules were found to have long aliphatic structures with many rotatable bonds. This reflects the fact that the databases were not prefiltered with respect to druglike properties. Given the wide-open active site and the fact that PR-ATP (MW 550 Da) is a cognate ligand, molecules heavier than average drugs were expected to bind. Many of the most promising hits from the docking were larger than 450 Da. In addition, charged or highly polar groups such as sulfates, sulfones, and nitriles were observed to bind in the PRPP binding site, which is expected to have affinitity for anionic groups (e.g., phosphates).

As a control, the reaction product PR-ATP was docked into the active site of the enzyme using GOLD and FlexX to ensure reliability of the programs. Both programs predicted similar binding conformations of the PR-ATP (see Figure 2). The phosphoribosyl group of PR-ATP interacts with the PRPP binding site, which is consistent with the partial crystal structure of PR-ATP in complex with *E. coli* ATP-PRTase.[7] The triphosphate group of PR-ATP interacted with the side chains of Arg49 and Lys51 near the ATP binding site.

On the basis of the initial ranking, 7000 compounds from the ChemBridge database and 4500 compounds from the NCI database (1−2% of each) were selected. To enhance fidelity, these compounds were redocked with greater thoroughness using FlexX. The top conformer of each was rescored using Consensus Scoring, which combines the FlexX score with four other energy functions (DOCK, PMF, ChemScore, and GOLD). Seven hundred compounds from the ChemBridge database had consensus scores of 4 or higher (representing how many out of the 5 scores for which the compound was ranked above the median), and 450 compounds were selected from the NCI database.

One-third of the top-ranked compounds were found to contain terminal or central sulfone groups making hydrogen bonds with backbone nitrogens of the nucleotide-binding loop (P-loop) or Ala139. The backbone nitrogen of residue Ala139, in combination with Asp154 and Glu141, has been proposed as a putative Mg^{2+}:PRPP binding site based on the observation of a sulfate ion in the apocrystal structure.[6] The sulfone groups in the docked

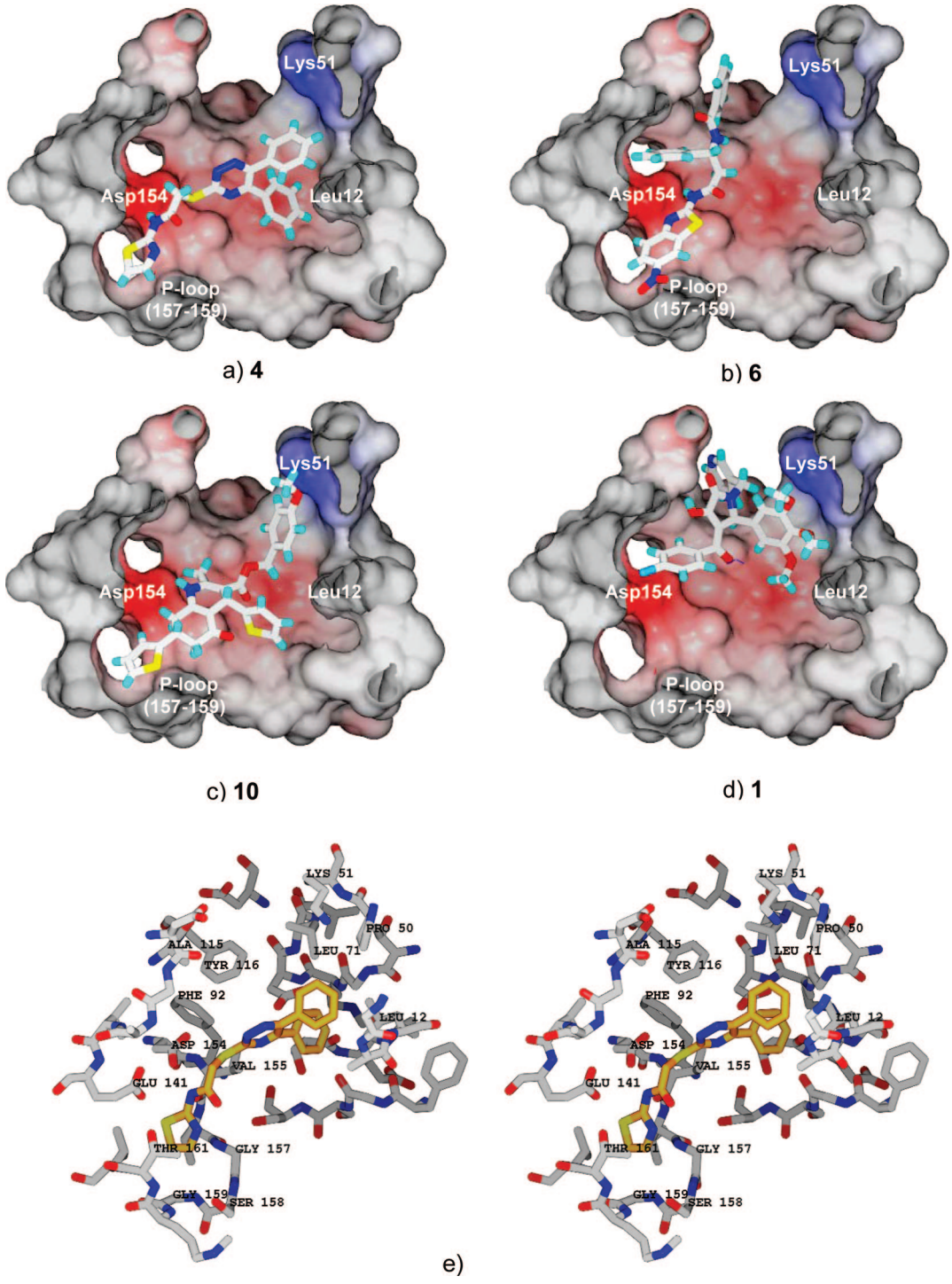

Figure 5. Surface representation of active site with four inhibitors bound in docked conformations: (a) **4**, (b) **6**, (c) **10**, and (d) **1**. (e) Repeat of docked conformation of **4** (a) in stereo, without surface, and with residues labeled to illustrate interactions.

compounds also interacted with two positively charged side chain residues, Arg59 and Lys51, from the other side of the cleft (domain I). Most of the hits make at least one hydrogen bond with Asp154 located at the center of the PRPP binding site.

Next, the hits were filtered by Lipinski's rules.[23] The Drug Discovery module of Cerius2 was used to calculate the descriptors corresponding to Lipinski's Rule of 5. Any molecule that violated more than half of the rules was rejected. In addition, molecules with more than eight rotatable bonds were eliminated. Because of the open nature of the active site, the limit on molecular weight was extended to 550 Da instead of the upper limit of 500 Da suggested by Lipinski. Using this filtering process, 154 out of the 700 compounds (22%) from the ChemBridge database and 90 out of the 450 (20%) from the NCI database were removed.

The remaining ~900 compounds were visually inspected using molecular graphics in Sybyl. Three primary binding modes were observed. Ligands bound to either one of the substrate binding sites (PRPP and ATP). In the third mode, they bound to the combined product-binding site (PR-ATP). A larger number of hits were found to bind the PRPP site than the other subsites. Negatively charged functional groups on the hits appeared to anchor the molecules to the oxyanion hole, as well

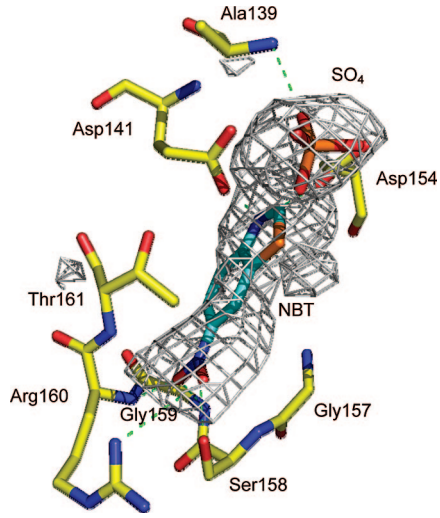

Figure 6. Electron density for crystal structure of complex with compound **6**. Partial density is observed for NBT moiety, along with a peak in the sulfate position.

as hydrogen-bonding with the carboxylate oxygens of residues Glu141 and Asp154. The molecules that docked to the ATP-binding site mainly interacted with either Arg49 and Lys51 or the hydrophobic pocket next to Leu12, Leu71, and Pro50. None of the hits occupied the entire active site as much as PR-ATP was predicted to contact. Nevertheless, instances of the third binding mode exhibit continuity from the PRPP binding site extending to the hydrophobic pocket of the ATP binding site.

Compounds were evaluated based on the following criteria: (1) potential for making hydrogen bonds with active site residues, (2) coverage of the active site, and (3) structural uniqueness (to avoid redundancy among chemically similar hits). Ultimately, 13 compounds from the ChemBridge database and 37 compounds from the NCI database were selected for in vitro testing (Figure 3 shows the ChemBridge selections).

In Vitro Assay of Inhibition Activity. Fifty compounds were tested for inhibition activity using an in vitro assay that monitored production of PR-ATP by the enzyme. A total of seven compounds showed appreciable inhibition at 10 μM (Figure 4). Three compounds, **4**, **6**, and **10**, exhibited greater than 50% inhibition at this concentration and were further diluted to find the minimal inhibitory concentration (MIC). Compounds **4** and **6** showed 40% and 35% inhibition of enzyme activity, respectively, even at 1 μM. The IC_{50}′s were estimated to be 4 μM for **4** and 6 μM for **6**. These can be converted to a K_i of approximately 2 μM by the Cheng and Prusoff equation, which is considerably better than that of known inhibitors such as dicoumarol (60 μM) and pentachlorophenol (50 μM).[14]

Predicted binding modes in the active site for four of the compounds are shown in Figure 5. One of the two phenyl groups of **4** interacts with the hydrophobic pocket formed by Leu12, Leu71, and Pro50 (Figure 5a). The central amide nitrogen hydrogen bonds with the side chain oxygen of Asp154 and the terminal thiazole ring is located close to the P-loop. The molecule spans the PR-ATP binding site, which is consistent with the highest inhibition profile among the top inhibitors.

In contrast, **6** occupies only the PRPP binding site (Figure 5b). The nitro group of its nitrobenzothiazole (NBT) moiety forms a tight hydrogen-bonding network with the backbone nitrogen atoms of the P-loop. The nitrogen atom in the thiazole ring and the amide nitrogen of its central peptide bond interact with the conserved Asp154 and contribute to stabilizing the molecule. The central phenyl ring is in the amphiphilic pocket near the middle of the PRPP binding site. The pendant phenyl ring appears to have no direct interaction with the active site.

Compound **10** also interacts with the PRPP binding site, but less strongly compared to **6**, according to the docking results (Figure 5c). In particular, the terminal thiophene ring was predicted to be close to the oxyanion hole of the P-loop, where negatively charged atoms are expected to interact. A ring nitrogen atom of the quinolone moiety in the center of the molecule also hydrogen bonds with Asp154. At the other end of the molecule, the ring portion of the methoxybenzyl group interacts with the hydrophobic pocket of the ATP binding site, while the ring oxygen hydrogen bonds with the side-chain nitrogen atom of Lys51.

Compound **1** was predicted to bind to the cavity between the domains I and II (Figure 5d). The terminal chlorobenzoyl group of **1** makes hydrophobic interactions with the amphiphilic pocket near the PRPP binding site. One of the trimethoxyphenyl oxygens hydrogen bonds to Lys51 in the ATP binding site. The pyridinylmethyl group binds to the hydrophobic surface just outside the cavity. Although this surface is possible for binding, it seems to be less able to block either substrate or product binding. This is consistent with the lowest order of inhibition among the top hits.

Exploration of Nitrobenzothiazole Functionality. The nitrobenzothiazole (NBT) substituent of **6** is intriguing because of its similarity to dinitrophenol, which has been shown to have inhibition activity against the *E. coli* HisG enzyme.[28] To examine the validity of the predicted binding of **6** in the active site, a co-crystal structure was determined from HisG apocrystals soaked with the inhibitor (see crystallographic statistics in Table S1, Supporting Information). The crystal diffracted to 2.9 Å and, after refinement, the *R*-factors were $R_{work} = 20\%$ and $R_{free} = 28\%$, respectively. No significant movements of backbone or side chain atoms were observed to be induced by ligand-binding. As in the apostructure, a strong peak in the density, likely due to a sulfate ion,[6] was observed near the backbone nitrogen of Ala139 and appeared to block access to the upper half of the PRPP binding site. However, clear density for the part of the inhibitor was observed in the Fourier difference map, starting from the oxyanion hole and continuing to the sulfate peak (Figure 6). This density is consistent with the size and shape of the NBT moiety, although density for the other groups (e.g., two phenyls) in the inhibitor would appear to conflict sterically with the sulfate ion and was not in fact observed. Attempts to screen for nonsulfate-containing crystallization conditions, to eliminate this potential steric conflict, were unsuccessful, and when the crystal was back-soaked in a solution without sulfate ion, the crystal exhibited serious anisotropic diffraction.

To identify additional compounds that might have activity based on these results, a search of the ChemBridge database was conducted for other compounds containing nitrobenzothiazole or structural analogues, yielding 4854 entries. These candidates were filtered by Lipinski′s Rules, using a maximum constraint violation of 10%, and then docked with FlexX and Consensus-scored in Sybyl. Protein−ligand interactions were examined for each of the successfully docked molecules. In particular, interactions made by atoms other than of the NBT moiety were scrutinized to determine whether they appear to contribute positively to the overall affinity of each molecule. After eliminating structural redundancies, 19 compounds were finally selected. Of these, four compounds showed inhibition in the enzyme assay against HisG at 10 μM: **17**−**20** (Figure 7). Compound **17** exhibited the highest inhibition (71%), followed

compound id		% Inh @ 10 μM	IC_{50}	LogP
17	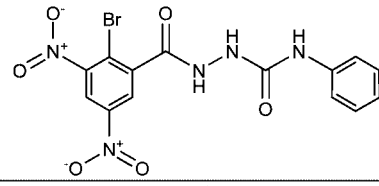	71%	5.5 μM	3.85
18	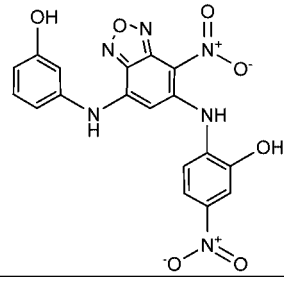	46%	11.9 μM	4.88
19	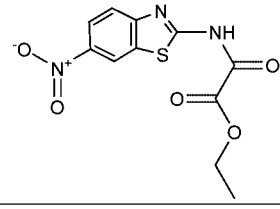	39%	13.9 μM	1.09
20	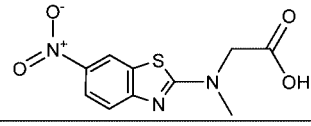	15%	n.d.	2.53

Figure 7. Structures of four compounds selected from ChemBridge library via similarity search to nitrobenzothiazole that showed significant enzyme inhibition activity. Estimates of hydrophobicity (logP) were derived from the ChemBridge Web site (http://hit2lead.com), except for **19**, which was obtained from the ZINC database (http://zinc.docking.org).

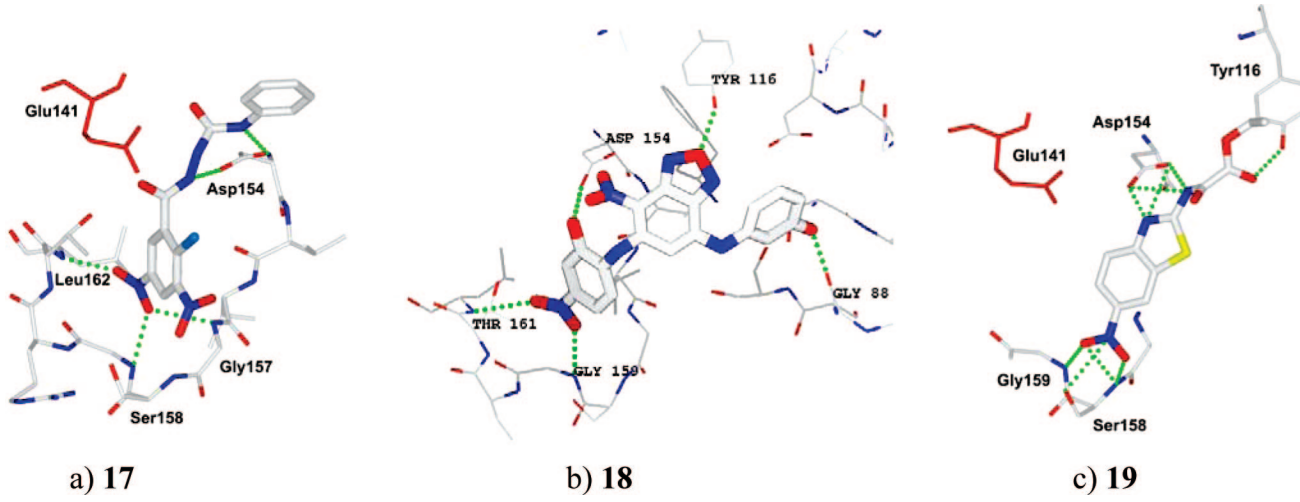

Figure 8. Docked conformations showing interactions with residues in the active site for compounds **17**, **18**, and **19** from the NBT-similarity screen. Potential hydrogen bonds (~3 Å) are shown in green.

by **18** (46%) and **19** (39%). IC_{50} values for three of these compounds were estimated as follows: 5.5 μM for **17**, 11.9 μM for **18**, and 13.9 μM for **19**.

Docked conformations for three of the compounds are shown in Figure 8, along with their interactions with residues in the active site. Compound **17** contains a brominated dinitro-phenyl group, rather than a benzothiazole (Figure 8a). One of the nitro groups hydrogen bonds to the backbone nitrogens of Gly157, Gly159, and Leu162, located deep in the P-loop, while the other apparently does not interact with protein. One nitrogen atom of the carboxamide group and the other nitrogen atom of the hydrazine group make hydrogen bonds with the conserved Asp154. These interactions seem to be critical for extending protein−ligand interactions beyond the oxyanion hole. In addition, **17** has a phenyl group connected by a polar linker that also appears to be important for the binding affinity of **6** (Figure 5b).

Compound **18** (Figure 8b) contains a nitrophenol group in place of the NBT of **6**, along with a benzoxadiazole component, which also contains a nitro group. The nitrophenol interacts with the P-loop, similar to **6**. The benzoxadiazole ring docks into the ATP-binding site and interacts with Tyr116. The hydroxyl

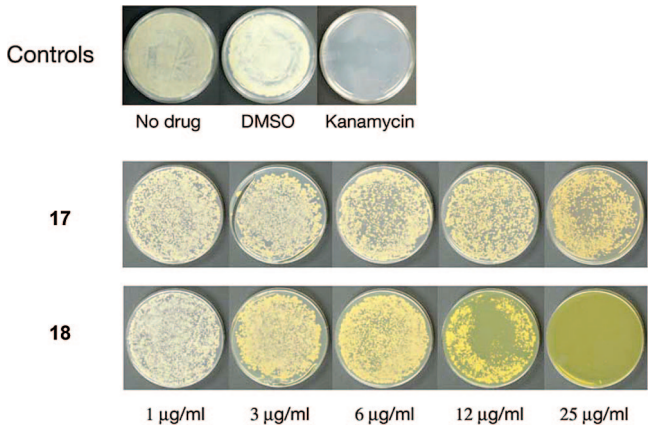

Figure 9. Whole-cell assay: inhibition of growth of *M. smegmatis*. Images of plates showing growth of cultures on full media, with varying concentrations of inhibitors applied.

group on the nitrophenol makes a hydrogen bond with Asp154. The terminal phenol group is stabilized by hydrogen bonding with the backbone oxygen of Gly88 and the side chain oxygen of Ser177 in the ATP-binding site.

Compound **19** has a nitrobenzothiazole group with an alkyl-ester tail (Figure 8c). It has a similar interaction profile as **6** for the NBT portion, although the nitro group hydrogen bonds to the backbone nitrogen of Ser158. In addition, an oxygen atom on the linear tail of **19** makes a unique hydrogen bond with the hydroxyl group of Tyr116. This possibly plays an important role for stability and specificity of the NBT moiety. Furthermore, the amide nitrogen next to the benzothiazole ring hydrogen bonds with one of the side chain oxygens of Asp154 and stabilizes both the benzothiazole ring and the linear chain.

Whole-Cell Activity in *M. smegmatis.* The compounds that showed inhibition in the enzyme assay were tested for bacteriocidal activity in a whole-cell assay with *M. smegmatis*. *M. smegmatis* is a mycobacterial strain with high genomic similarity to *M. tuberculosis*, making it a good surrogate for testing in vivo activity of potential inhibitors. Like *M. tuberculosis*, *M. smegmatis* has a thick outer cell wall with extremely long-chain fatty acids ($\sim C_{60}$ mycolates) to help protect it against the host−cell defenses inside macrophages, thus reducing permeability of many small molecule. Cultures of *M. smegmatis* were mixed with each compound in concentrations ranging from 1−25 μg/mL and plated. After 4 days, the plates were inspected for growth. A plate with no inhibitors and one with DMSO were used as negative controls, and a plate with 25 μg/mL of kanamycin was used as a positive control (because the strain of *M. smegmatis* used was kanamycin-sensitive).

Two of the compounds demonstrated inhibition of bacterial growth (Figure 9). Compound **17** weakly inhibited growth at 25 μg/mL. Compound **18** exhibited significant growth inhibition at 12 μg/mL and 100% inhibition at 25 μg/mL. These two compounds contain nitroaryl moieties similar to nitrobenzothiazole. It should also be noted that the logP is predicted to be higher for **17** and **18** than for the other two compounds showing enzyme activity but not whole-cell activity (Figure 7). These observations are consistent with recent studies of molecular properties among known inhibitors with antitubercular activity, which have been observed to have slightly higher logP values than typical oral drugs, possibly needed to facilitate passive diffusion across the thicker mycobacterial cell wall.[29]

Conclusion

Virtual screening was carried out to identify novel inhibitors for *M. tuberculosis* HisG. Using both GOLD and FlexX, over 500000 compounds were docked and ranked by Consensus-scoring. Fifty compounds were initially selected for testing, and of these, seven were found to have inhibition activity in an enzyme assay, with five compounds having IC_{50}'s at or below 10 μM. Distributed computing was an essential component of the methodology that enabled screening of such large databases in a reasonable amount of time, affording the potential benefit of yielding more diverse hits than would be possible by the more traditional approach of doing focused screens based on known scaffolds. However, visual inspection also played an important role in selecting compounds (among those most highly ranked) that appeared to make the most favorable interactions with the active site (in their docked conformations). Despite many concerns frequently voiced about virtual screening (e.g., adequacy of conformation sampling, accuracy of scoring functions, etc.), the methodology has been demonstrated to work well, yielding 11 μM inhibitors out of a total of 69 compounds tested (including those from a secondary screen). The most potent compound, **4**, had an IC_{50} of 4 μM, and compounds with even higher potency could eventually be identified that are based on analogues of the compounds described in this paper as a starting point.

The most interesting scaffold discovered in this effort was nitrobenzothiazole (NBT). This scaffold is reminiscent of dinitrophenol, which has weak inhibition activity against *E. coli* HisG (0.4 mM). The compounds found by virtual screening were much more potent. A secondary virtual screen was performed to select compounds from the libraries that bore similarity to the initial hit containing NBT. Among the combined set of compounds that were found to have enzyme inhibition activity in this study, 3 out of 11 compounds contained NBT as a substituent. All three compounds (as well as other nitro-aryl compounds) docked to the PRPP-binding region of the active site, with the nitro groups generally interacting with backbone and side chain atoms in the P-loop (via hydrogen bonds). This predicted protein−ligand interaction was confirmed crystallographically for one of the hits containing NBT (**6**), which showed electron density in this position in the Fourier-difference map for a co-crystal produced by soaking.

Two compounds identified by the virtual screen were also shown to have whole-cell activity against *M. smegmatis*: **17** (25 μM MIC) and **18** (12 μM MIC), although both of these compounds contained nitro-aryl groups rather than nitrobenzothiazole. Pending further studies (e.g., target validation, ADME/T analysis, etc.), these compounds (or more potent analogs of them) could be considered as candidates for development into novel drugs against tuberculosis.

Acknowledgment. This work was supported by National Institutes of Health grant P01-AI068135 and by the Robert A. Welch Foundation (A-0015).

Supporting Information Available: Crystallographic data. This material is available free of charge via the Internet at http://pubs.acs.org.

References

(1) Alfiano, P.; Fani, R.; Lio, P.; Lazcano, A.; Bazzicalupo, M.; Carlomagno, M. S.; Bruni, C. B. Histidine biosynthetic pathway and genes structure, regulation and evolution. *Microbiol. Rev.* **1996**, *60*, 44–69.

(2) Centers for Diseases Control. Emergence of *Mycobacterium tuberculosis* with extensive resistance to second-line drugs-worldwide 2000−2004. *Morbidity and Mortality Weekly Report* **2006**, *55*, 301−305.

(3) Sassetti, C. M.; Boyd, D. H.; Rubin, E. J. Comprehensive identification of conditionally essential genes in mycobacteria. *Proc. Natl. Acad. Sci. U.S.A.* **2001**, *98*, 12712–12717.

(4) Parish, T. Starvation survival response of *Mycobacterium tuberculosis*. *J. Bacteriol.* **2003**, *185*, 6702–6706.
(5) Betts, J. C.; Lukey, P. T.; Robb, L. C.; McAdam, R. A.; Duncan, K. Evaluation of a nutrient starvation model of *Mycobacterium tuberculosis* persistence by gene and protein expression profiling. *Mol. Microbiol.* **2002**, *43*, 717–731.
(6) Cho, Y.; Sharma, V.; Sacchettini, J. C. Crystal structure of ATP phosphoribosyltransferase from *Mycobacterium tuberculosis*. *J. Biol. Chem.* **2003**, *278*, 8333–8339.
(7) Lohkamp, B.; McDermott, G.; Campbell, S. A.; Coggins, J. R.; Lapthorn, A. J. The structure of *Escherichia coli* ATP-phosphoribosyltransferase. Identification of substrate binding sites and mode of AMP inhibition. *J. Mol. Biol.* **2004**, *336*, 131–144.
(8) Champagne, K. S.; Sissler, M.; Larrabee, Y.; Doublié, S.; Francklyn, C. S. Activation of the hetero-octameric ATP phosphoribosyl transferase through subunit interface rearrangement by a tRNA synthetase paralog. *J. Biol. Chem.* **2005**, *280*, 34096–34104.
(9) Vega, M. C.; Zou, P.; Fernandez, F. J.; Murphy, G. E.; Sterner, R.; Popov, A.; Wilmanns, M. Regulation of the hetero-octameric ATP phosphoribosyl transferase complex from *Thermotoga maritima* by a tRNA synthetase-like subunit. *Mol. Microbiol.* **2005**, *55*, 675–686.
(10) Schramm, V. L.; Grubmeyer, C. Phosphoribosyltransferase mechanisms and roles in nucleic acid metabolism. *Prog. Nucleic Acid Res. Mol. Biol.* **2004**, *78*, 261–304.
(11) Morton, D. P.; Parsons, S. M. Biosynthetic direction substrate kinetics and product inhibition studies on the first enzyme of histidine biosynthesis, adenosine triphosphate phosphoribosyltransferase. *Arch. Biochem. Biophys.* **1976**, *175*, 677–686.
(12) Champagne, K. S.; Piscitelli, E.; Francklyn, C. S. Substrate recognition by the hetero-octameric ATP phosphoribosyltransferase from *Lactococcus lactis*. *Biochemistry* **2006**, *45*, 14933–14943.
(13) Morton, D. P.; Parsons, S. M. Inhibition of ATP phosphoribosyltransferase by AMP and ADP in the absence and presence of histidine. *Arch. Biochem. Biophys.* **1977**, *181*, 643–648.
(14) Dall-Larsen, T.; Kryvi, H.; Klungsoyr, L. Dinitrophenol, dicoumarol and pentachlorophenol as inhibitors and parasite substrates in the ATP phosphoribosyltransferase reaction. *Eur. J. Biochem.* **1976**, *66*, 443–446.
(15) Gohda, K.; Ohta, D.; Kozaki, A.; Fujimori, K.; Mori, I.; Kikuchi, T. Identification of novel potent inhibitors for ATP-phosphoribosyl transferase using three-dimensional structural database search technique. *Quant. Struct.−Act. Relat.* **2001**, *20*, 143–147.
(16) Verdonk, M. L.; Cole, J. C.; Hartshorn, M. J.; Murray, C. W.; Taylor, R. D. Improved protein−ligand docking using GOLD. *Proteins* **2003**, *52*, 609–623.
(17) Kramer, B.; Rarey, M.; Lengauer, T. Evaluation of the FlexX incremental construction algorithm for protein−ligand docking. *Proteins: Struct., Funct., Genet.* **1999**, *37*, 228–241.
(18) Meng, E. C.; Shoichet, B. K.; Kuntz, I. D. Automated docking with grid-based energy evaluation. *J. Comput. Chem.* **1992**, *13*, 505–524.
(19) Eldridge, M. D.; Murray, C. W.; Auton, T. R.; Paolini, G. V.; Mee, R. P. Empirical scoring functions. Part I. The development of a fast empirical scoring function to estimate the binding affinity of ligands in receptor complexes. *J. Comput.-Aided Mol. Des.* **1997**, *11*, 425–445.
(20) Muegge, I.; Martin, Y. C. A general and fast scoring function for protein−ligand interactions: a simplified potential approach. *J. Med. Chem.* **1999**, *42*, 791–804.
(21) Jones, G.; Willett, P.; Glen, R. C.; Leach, A. R.; Taylor, R. Development and validation of a genetic algorithm for flexible docking. *J. Mol. Biol.* **1997**, *267*, 727–748.
(22) Clark, R. D.; Strizhev, A.; Leonard, J. M.; Blake, J. F.; Matthew, J. B. Consensus scoring for ligand/protein interactions. *J. Mol. Graph. Model.* **2002**, *20*, 281–295.
(23) Lipinski, C. A.; Lombardo, F.; Dominy, B. W.; Feeney, P. J. Experimental and computational approaches to estimate solubility and permeability in drug discovery and development settings. *Adv. Drug Delivery Rev.* **2001**, *46*, 3–26.
(24) Otwinowski, Z.; Minor, W. Processing of X-ray Diffraction Data Collected in Oscillation Mode. In *Methods in Enzymology: Volume 276: Macromolecular Crystallography, Part A*; Carter, C. W., Sweet, R. M. Eds.; Academic Press.; New York, 1997; pp 307−326.
(25) Storoni, L. C.; McCoy, A. J.; Read, R. J. Likelihood-enhanced fast rotation functions. *Acta Crystallogr., Sect. D: Biol. Crystallogr.* **2004**, *60*, 432–438.
(26) Brünger, A. T.; Adams, P. D.; Clore, G. M.; DeLano, W. L.; Gros, P.; Grosse.Kunstleve, R. W.; Jiang, J. S.; Kuszewski, J.; Nilges, M.; Pannu, N. S.; Read, R. J.; Rice, L. M.; Simonson, T.; Warren, G. L. Crystallography & NMR system: A new software suite for macromolecular structure determination. *Acta Crystallogr., Sect. D: Biol. Crystallogr.* **1998**, *54*, 905–921.
(27) Murshudov, G. N.; Vagin, A. A.; Dodson, E. J. Refinement of macromolecular structures by the maximum-likelihood method. *Acta Crystallogr., Sect. D: Biol. Crystallogr.* **1997**, *53*, 240–255.
(28) Dall-Larsen, T.; Fasold, H.; Klungsoyr, L.; Kryvi, H.; Meyer, C.; Ortanderl, F. Affinity labelling to−SH groups in adenosine triphosphate phosphoribosyl transferase with the dinitrophenyl group from *S*-dinitrophenyl-6-mercaptopurine-riboside 5′-phosphate. *Eur. J. Biochem.* **1975**, *60*, 103–107.
(29) Barry, C.E., III; Slayden, R. A.; Sampson, A. E.; Lee, R. E. Use of genomics and combinatorial chemistry in the development of new antimycobacterial drugs. *Biochem. Pharmacol.* **2000**, *59*, 221–231.

JM800328V